

# Shared Latent Space of Font Shapes and Impressions

Jihun Kang<sup>1</sup>, Daichi Haraguchi<sup>1</sup>, Akisato Kimura<sup>2</sup>, and Seiichi Uchida<sup>1</sup>  
<sup>1</sup> Kyushu University, Fukuoka, Japan {kang.jihun}@human.ait.kyushu-u.ac.jp  
<sup>2</sup> NTT Communication Science Laboratories, NTT Corporation, Japan

**Abstract.** We have specific impressions from the style of a typeface (font), suggesting that there are correlations between font shape and its impressions. Based on this hypothesis, we realize a shared latent space where a font shape image and its impression words are embedded in a cross-modal manner. This latent space is useful to understand the style-impression correlation and generate font images by specifying several impression words. Experimental results with a large style-impression dataset prove that it is possible to accurately realize the shared latent space, especially for shape-relevant impression words, and then use the space to generate font images with various impressions.

**Keywords:** Font shape · Font impression · Shared latent space.

## 1 Introduction

It is known that different font shapes give different impressions. A recent paper [4] provides a large font dataset, where many people attach impression words to individual fonts. Fig. 1 shows several examples of fonts and their impressions. In the dataset, 1,824 impression words are attached to the 18,815 fonts; therefore, about 10 different impression words are attached to each font on average.

This fact suggests that font is a multi-modal medium. A font is presented as letter images, i.e., visible shapes; simultaneously, it gives various impressions. If we can believe that the impression can be represented by a set of words, like Fig. 1, the multi-modality of a specific font is defined as the pairwise relationship between “a shape set” and “an impression word set.” For example, the font **4-square** has two modalities, the 52 shape images of ‘A’ to ‘z’ and a set of impression words {heavy, headline, display, . . .}.

Our research aims to construct a latent space representing semantics shared with the two modalities, i.e., font images and their impressions, to understand the relationship between them. This latent space enables cross-modal translations; we can describe a given font image with appropriate impression words and search for or even generate font images for a given set of impression words through the obtained latent space. Fig. 2 illustrates the idea of the shared latent space. Let  $\mathbf{X}_i$  denote the  $i$ -th font (i.e., a set of images from ‘A’ to ‘Z’ of the  $i$ -th font) and assume a set of  $J_i$  impression words  $\mathbf{W}_i = \{w_{i,1}, \dots, w_{i,j}, \dots, w_{i,J_i}\}$  are attached to the font  $\mathbf{X}_i$ . In the  $d$ -dimensional shared latent space, we expect

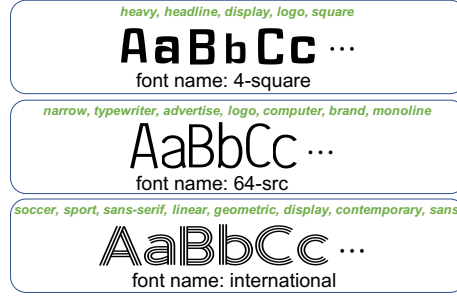


**Fig. 1.** Examples of font images with their impression words.

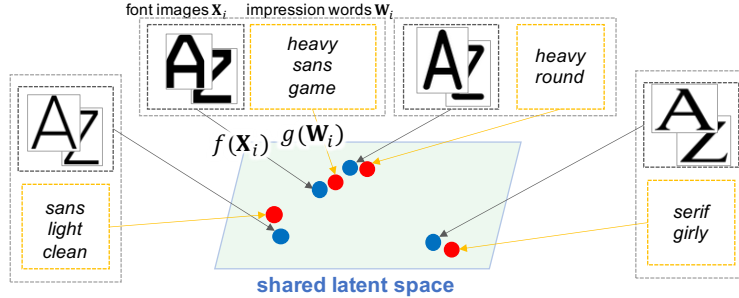


**Fig. 2.** The goal of our research: constructing a latent space representing semantics shared with font images and their impressions.

that  $f(\mathbf{X}_i) \sim g(\mathbf{W}_i)$  for all  $i$ , where the functions  $f$  and  $g$  give  $d$ -dimensional representations of  $\mathbf{X}_i$  and  $\mathbf{W}_i$ , respectively. Therefore, the realization of the latent space is the task of getting the representation functions  $f$  and  $g$  that satisfy this proximity condition.

This paper proposes a novel machine learning-based analysis framework, as shown in Fig. 3, for constructing a shared latent space. We rely on a *cross-modal* network structure, where two modalities  $\mathbf{X}_i$  and  $\mathbf{W}_i$  are fed to two neural networks that realize  $f$  and  $g$ , respectively. Those two neural networks are co-trained to build a shared latent space. In order to guarantee that the representations  $f(\mathbf{X}_i)$  and  $g(\mathbf{W}_i)$  still keep the original information carried by  $\mathbf{X}_i$  and  $\mathbf{W}_i$ , our framework employs an auto-encoder for each modality.

In the proposed framework, we employ DeepSets [26], which can deal with sets as the input. The word set  $\mathbf{W}_i$  will have an arbitrary number  $J_i$  of impression words and thus cannot deal with a standard data input scheme. As shown in Fig. 4, DeepSets first converts  $J_i$  elements  $w_{i,1}, \dots, w_{i,j}, \dots, w_{i,J_i}$  of  $\mathbf{W}_i$  as  $J_i$  feature vectors  $e(w_{i,1}), \dots, e(w_{i,j}), \dots, e(w_{i,J_i})$  independently and then average them into a single  $d$ -dimensional vector  $h(\mathbf{W}_i) = \sum_j e(w_{i,j})/J_i$ . This simple procedure allows us to deal with an arbitrary number of the set elements, while avoiding the effect of the order of elements.

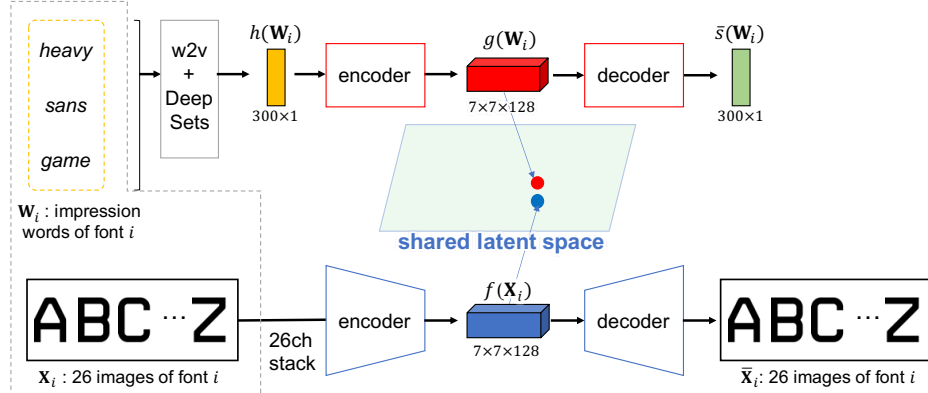


**Fig. 3.** Overview of the proposed method to generate the latent space shared by two totally different modalities, that is, font shape images and their impression words.

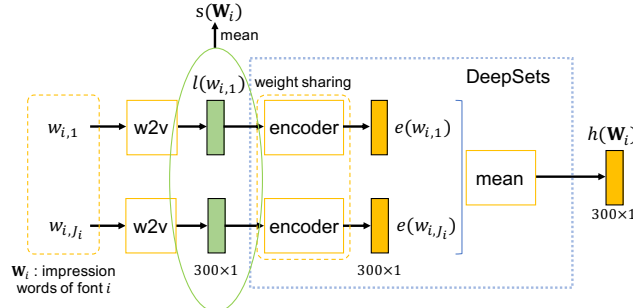


**Fig. 4.** Word vector by aggregating the word vectors of multiple impression words by word2vec and DeepSets.

If the shared latent space is realized, there are several possible applications. Fig. 5 shows two main applications; (a) font image retrieval and (b) font image generation. In both applications, we can specify an arbitrary number of impression words. Then, (a) existing font images and (b) new font images are provided with the specified impressions, respectively.

We have to note that the proposed method based on DeepSets also allows us to understand the shape-relevance of the individual words. A careful observation of Fig. 1 implies that there are two types of impression words: *shape-relevant* and *shape-irrelevant*. The former is the impression words that are understandable from the font shape. For example, the impression words, such as *sans-serif* and *heavy*, are shape-relevant. The latter, shape-irrelevant words, is not understandable from the font shape. For example, *soccer* attached to the font *international* in Fig. 1 is not understandable without knowing the font is used for the uniform of a soccer team.

Based on the above discussions, we can summarize the main technical contributions of this paper as follows:

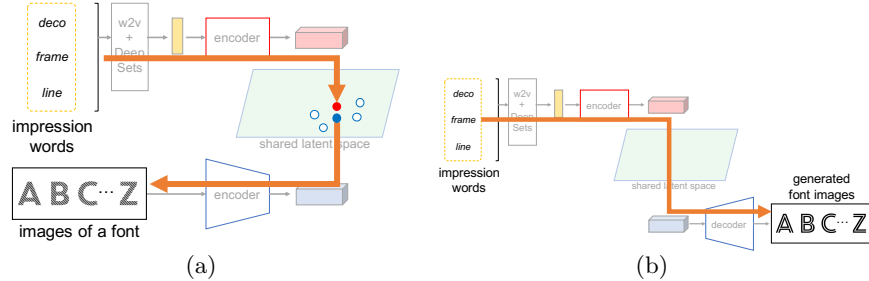


**Fig. 5.** Possible applications of the shared latent space. (a) Font image retrieval. (b) Font image generation.

- The proposed method can construct latent space representing semantics shared with font image and their impression words. By doing this, we can capture the relationship between font shapes or styles and impression words through the latent space.
- The latent space derived by the proposed method is generic. It can be applied to various downstream tasks, such as font image retrieval and generation with impression words.

## 2 Related Work

### 2.1 Font style and impression

Fonts affect some impressions to readers. In the fields of psychology and marketing, the relationship between fonts and the impressions has been analyzed experimentally for long years [5,7,12,17]. For instance, Doyle et al. [7] have reported that fonts affected the perception of the brand name.

In recent years, the relationship between font styles and various targets concerning impressions has been analyzed, and font recommendation systems corresponding impressions of targets have been proposed. Shinahara et al. [18] have analyzed the relationship between font styles and genre in book and advertisement. Choi et al. [6] and Shirani et al. [19] develop font recommendation systems; they select fonts that match the impressions of images and texts, respectively. O'Donovan et al. [15] have published a dataset with 200 different fonts, each of which is annotated with the degrees of 37 attributes. Chen et al. [4] published a far larger collection of fonts tagged with impression words and proposed a font retrieval method using word queries.

Font style classification and identification are other important tasks for dealing with fonts. Font style classification, such as [27], is a task to classify a font image to one of the styles, such as roman, slant, bold, serif, sans-serif, etc. Font identification is a task to estimate the name of the font family, such as **Helvetica**, from images. DeepFont has been proposed [25] for this purpose. Haraguchi et al. [9] tackle the font identification task as a matching problem.

As an extension of various GAN-based font image generation, such as [10,13], generation of font images with specific impressions has been recently examined by Wang et al. [24]. Their Attribute2Font uses the dataset teodonovan to generates fonts by specifying the degrees of 37 attributes, such as *gentle* and *fresh*.

Those font recommendation, search, style classification, and generation methods are developed in a more application-oriented manner and do not focus on the essential correlation between font styles and the impressions; therefore, they do not deal with the shared latent space. To the authors' best knowledge, this is the first attempt to prove that the letter images  $\mathbf{X}_i$  and the impression words  $\mathbf{W}_i$  of the  $i$ th font can be embedded into the same  $d$ -dimensional vector space to satisfy  $f(\mathbf{X}_i) \sim g(\mathbf{W}_i)$  as possible for all  $i$ .

## 2.2 Latent space embedding

In multimodal modeling of images and texts, many attempts have been made for shared latent space embedding of the images and texts. Socher et al. [20] have proposed a model that segments and annotates images by mapping images associated with the words to a latent semantic space. The same group extended this idea [21] by incorporating a neural network-based representation learning scheme of the image modality. In this work, the text modality is encoded by a hand-crafted feature, and then the image modality is mapped to the fixed text modality. In the works focusing on neural language caption generation [8,11,23], images and texts are not embedded into the same latent space explicitly, but image features by Convolutional Neural Networks (CNNs) are used as an input of Recurrent Neural Networks (RNNs) that generate textual information.

In the document analysis research field, Almazán et al. [1] have published a pioneering work that a word image and its textual information are embedded into the same space for word spotting and recognition even in a zero-shot manner. Such an embedding strategy is nowadays extended to deal with a tough multimodal task, called Text VQA [2]. Sumi et al. [22] realized a shared latent space between online and offline handwriting sample pairs and proved that a stroke order recovery is possible via the shared latent space.

## 2.3 Representation learning for a set

When each training sample comprises a different number of elements without any specific order, some machine learning architecture that accepts a set as its input sample is necessary. DeepSets [26] has been proposed a simple but powerful framework to deal with sets as samples. As shown in Fig. 4, DeepSets treats the elements in an input set independently during its feature extraction layer and then combines the feature vectors into a single vector by a simple operation, such as sum, average, and max. In recent years, Saito et al. [16] have proposed the architecture to use sets by capturing the properties from the basis of set matching mathematically and have tried novel fashion item matching using sets.

In this paper, we treat the impression words  $\mathbf{W}_i$  attached to the  $i$ th font as a set. The number of the attached words is different among fonts, as shown in

Fig. 1. In addition, the words have no specific order. We, therefore, use DeepSets to treat  $\mathbf{W}_i$  as a set. Note that the other modality  $\mathbf{X}_i$  is also comprised of 26 images (from ‘A’ to ‘Z’) and possible to deal with a set; however, in our setup,  $\|\mathbf{X}_i\|$  is always 26 and the order of the 26 images is better to be fixed in alphabetical order. Therefore, we represent  $\mathbf{X}_i$  as a stack of 26 images.

### 3 MyFonts dataset [4]

As the font dataset with impression words, we employ the dataset published by Chen et al., [4]. This dataset, hereafter called the MyFonts dataset, comprises 18,815 fonts collected at [MyFonts.com](http://MyFonts.com). As shown in Fig. 1, each font is tagged with  $0 \sim 184$  impression words attached by crowd-sourcing. This means that the impression words have a large variability according to the crowd-sourcing workers’ subjective bias. The vocabulary size of the impression words is 1,824. As noted in Section 1, most impression words are shape-relevant, but some are independent of shapes, such as *soccer*. (Recall that the bottom example of Fig. 1 has this word.)

Since we need to train several networks as a function  $g(\cdot)$  with sufficient samples, we removed non-frequent impression words attached to less than 100 fonts. Consequently, we used 451 impression words in our experiments. In addition, we removed the dingbat (pictorial symbols) fonts and the circled fonts from the MyFonts dataset by manual inspections by three persons. We also removed fonts without any impression words (after the above non-frequent word removal). Consequently, we used 9,980, 2,992, and 1,223 fonts for training, validating, and testing, respectively. Hereafter  $\Omega_{\text{train}}$ ,  $\Omega_{\text{val}}$  and  $\Omega_{\text{test}}$  denote the training, validation, and test font sets, respectively. Note that we used capital letter images of ‘A’ to ‘Z’ in each font.

## 4 Shared Latent Space of Font Shape and Impression

This section provides the method to train our model of Fig. 3 to realize a shared latent space. The training is organized in a two-step manner for faster and more accurate convergence. We first perform two independent training pipelines as an initialization of the cross-modal encoding scheme. More specifically, we independently train two different autoencoders for font shapes (the bottom pipeline of Fig. 3) and impression word (the upper pipeline). The latent vectors of those autoencoders correspond to  $f(\mathbf{X}_i)$  and  $g(\mathbf{W}_i)$ , respectively. Second, the end-to-end co-training will be performed to embed those latent vectors into the shared space to satisfy the condition  $f(\mathbf{X}_i) \sim g(\mathbf{W}_i)$ .

### 4.1 Font shape encoding by autoencoder and its initialization

An autoencoder is used for generating the latent vector  $f(\mathbf{X}_i)$  of the image modality, i.e., font shapes. As shown in the bottom part of Fig. 3, the autoencoder accept  $\mathbf{X}_i$  as its input and generate  $\bar{\mathbf{X}}_i$  via an intermediate compressed

representation  $f(\mathbf{X}_i)$ . Both of  $\mathbf{X}_i$  and  $\bar{\mathbf{X}}_i$  are 26 images (stacked as 26 channels) and expected to be similar with each other, i.e.,  $\mathbf{X}_i \sim \bar{\mathbf{X}}_i$ , in order to guarantee that  $f(\mathbf{X}_i)$  carries the original shape information of  $\mathbf{X}_i$  sufficiently. Note that  $f(\mathbf{X}_i)$  is emitted from the autoencoder as a tensor of  $7 \times 7 \times 128$ , whereas it is flattened as a  $d = 7 \times 7 \times 128 = 6,272$ -dimensional vector in the shared latent space. In the following, these two representations are not distinguished unless otherwise mentioned ( $g(\mathbf{W}_i)$  also).

The encoder ( $\mathbf{X}_i \mapsto f(\mathbf{X}_i)$ ) is based on ResNet18 (pre-trained with ImageNet) and the decoder ( $f(\mathbf{X}_i) \mapsto \bar{\mathbf{X}}_i$ ) is comprised of several deconvolutional layers. (See Section 5.1 for the detail.) They are trained to minimize the following construction loss function  $L_{\text{shape}}$ :

$$L_{\text{shape}} = \sum_{i=1}^N \|\mathbf{X}_i - \bar{\mathbf{X}}_i\|, \quad (1)$$

where  $N$  is the number of fonts used for training.

It is possible to initialize the autoencoder for the image modality by using font images  $\mathbf{X}_i \in \Omega_{\text{train}}$ , independently of the text modality. Specifically, the encoder and the decoder are trained to minimize  $L_{\text{shape}}$  for  $\{\mathbf{X}_i\}$ . Note that the autoencoder of the text modality will not be pre-trained, as described later.

## 4.2 Impression word encoding by Word2vec and DeepSets and their initialization

Like the image modality, an autoencoder is used for generating the impression word vectors  $g(\mathbf{W}_i)$ . However, the text modality requires extra modules to accept an arbitrary number of impression words  $\mathbf{W}_i = \{w_{i,1}, \dots, w_{i,j}, \dots, w_{i,J_i}\}$  as its input. Moreover, each impression word  $w_{i,j}$  should be converted to a semantic vector, so that similar impression words give similar effects to the system. Therefore, before the autoencoder the impression word  $w_{i,j}$  is converted to a semantic vector  $l(w_{i,j})$  by Word2vec [14] and then in the front-end of the autoencoder, all the semantic vectors are aggregated to a single fixed-dimensional vector  $h(\mathbf{W}_i)$  by DeepSets [26]. We treat  $s(\mathbf{W}_i) = \sum_j l(w_{i,j})/J_i$  as the original vector representing the  $J_i$  impression words and extract the latent vector  $g(\mathbf{W}_i)$  from it by an encoder.

Word2vec is a well-known word embedding method<sup>3</sup> that generates a fixed-dimensional vector  $l(w_{i,j})$  for a word  $w_{i,j}$ . If a pair of words  $w_{i,j}$  and  $w_{i,j'}$  have similar meanings (like *bold* and *thick*), we expect  $l(w_{i,j}) \sim l(w_{i,j'})$ . Although the one-hot representation might be a simpler choice, we use the word embedding method since we can expect that the semantically-similar impression words give a similar effect on  $g(\mathbf{W}_i)$ . We use word2vec pretrained by Google News dataset and do not retrain it by our dataset.

---

<sup>3</sup> If necessary, it is possible to use an arbitrary word embedding methods, such as fasttext [3] and other pre-trained models.

The  $J_i$  semantic vectors  $\{l(w_{i,j})|j = 1, \dots, J_i\}$  are then converted into a single vector  $h(\mathbf{W}_i)$  by DeepSets. As shown in Fig. 4, DeepSets has two functions: a trainable encoding scheme, or representation learning, and an aggregation scheme. The former is a deep neural network and gives a new representation  $e(w_{i,j})$  for the word2vec vector  $l(w_{i,j})$ . The later is the simple averaging process  $h(\mathbf{W}_i) = \sum_j e(w_{i,j})/J_i$ , whereas DeepSets can employ another pooling process, such as sum and max.

The encoder ( $s(\mathbf{W}_i) \mapsto g(\mathbf{W}_i)$ ) is ResNet18 (with random initialization) and the decoder ( $g(\mathbf{W}_i) \mapsto \bar{s}(\mathbf{W}_i)$ ) is composed of several fully-connected layers (see Section 5.1 for the detail). Specifically, the encoder and the decoder are trained by minimizing the following loss function:

$$L_{\text{impression}} = \sum_{i=1}^N \|s(\mathbf{W}_i) - \bar{s}(\mathbf{W}_i)\|. \quad (2)$$

One might think that we can skip the encoder in DeepSets, that is, it might be possible to use the averaged word2vec vectors  $s(\mathbf{W}_i)$  directly as  $h(\mathbf{W}_i)$ . However, the two-step encoding scheme via DeepSets is necessary. The first encoder in DeepSets plays the role of suppressing the effect of shape-irrelevant words by setting their vectors smaller. Then, the second encoder will convert  $h(\mathbf{W}_i)$ , which mainly carries the information of shape-relevant impression words, into the latent vector  $g(\mathbf{W}_i)$ , which is expected to be similar to the font shape vector  $f(\mathbf{X}_i)$ .

Like the image modality, we can initialize this pipeline (i.e., the autoencoder and DeepSets) independently by minimizing the loss function  $L_{\text{impression}}$ . Note that we cannot initialize the pipeline by using  $h(\mathbf{W}_i)$  instead of  $s(\mathbf{W}_i)$ . This is because it results in the trivial solution that  $h(\mathbf{W}_i) \equiv \bar{h}(\mathbf{W}_i) \equiv 0$  by abusing the encoder inside DeepSets.

### 4.3 Co-training for the shared latent space

After the pre-training of the autoencoder for both modality, all the modules of both modalities are co-trained to realize the shared latent space. From its purpose to have  $f(\mathbf{X}_i) \sim g(\mathbf{W}_i)$ , we have the following loss function:

$$L_{\text{share}} = \sum_{i=1}^N \|f(\mathbf{X}_i) - g(\mathbf{W}_i)\|. \quad (3)$$

Consequently, the overall loss function  $L$  of the proposed method becomes:

$$L = L_{\text{shape}} + L_{\text{impression}} + L_{\text{share}}. \quad (4)$$

In the process of minimizing the loss function  $L$ , the weights of all autoencoders and DeepSets are trained simultaneously.

*serif, modern, sans-serif, text, magazine, elegant, book, slab-serif, humanist, fashion, ultra-bold, editorial, contemporary, signage, bold, clean, poster, condense*

**Fig. 6.** 18 words with  $P@10 \geq 0.5$ .

## 5 Experimental Results

### 5.1 Implementation details

For the image modality, the encoder ( $\mathbf{X}_i \mapsto f(\mathbf{X}_i)$ ) is ResNet18 (pre-trained by ImageNet) that have additional convolution layer whose kernel size is  $1 \times 1$  and number of channel is 128. The decoder ( $f(\mathbf{X}_i) \mapsto \bar{\mathbf{X}}_i$ ) is  $D_{(512,1,0)}^{1 \times 1} - R - D_{(256,2,1)}^{4 \times 4} - R - D_{(128,2,1)}^{4 \times 4} - R - D_{(64,2,1)}^{4 \times 4} - R - D_{(32,2,1)}^{4 \times 4} - R - D_{(26,2,1)}^{4 \times 4}$  where D and R show transpose convolution layer and Relu function respectively. The parenthesized description shows (channels, stride, padding) and the superscript shows the kernel size.

For the text (impression word) modality, the encoder ( $h(\mathbf{W}_i) \mapsto g(\mathbf{W}_i)$ ) is  $F_{(1024)} - R - F_{(2048)} - R - F_{(6272)}$ , and the decoder ( $g(\mathbf{W}_i) \mapsto \bar{s}(\mathbf{W}_i)$ ) is  $F_{(2048)} - R - F_{(1024)} - R - F_{(300)}$  where F shows fully-connected layer. Note that the parenthesized description shows hidden units.

The entire network is trained by the training font set  $\Omega_{\text{train}}$  (9,980 fonts) and tested by the test set  $\Omega_{\text{test}}$  (1,223 fonts). The hyper-parameters and the training epochs are optimized by  $\Omega_{\text{val}}$  (2,992 fonts).

### 5.2 Qualitative evaluation 1: Observing the shared latent space via a font image retrieval task

As shown in Fig. 5 (a), the proposed shared latent space can be used for font image retrieval by the query of impression words. In this section, we conduct the retrieval experiment by using the test dataset  $\Omega_{\text{test}}$ , to understand the characteristics of the learned latent space. Especially, we carefully observe the difference between shape-relevant impression words and shape-irrelevant impression words through this experiment.

Fig. 6 shows the impression words with higher  $P@K$  values.  $P@K$  (abbreviation of “Precision at  $K$ ”) of a word  $w$  is a metric for the information retrieval task. In our task, it evaluates how many the font shapes with the same word  $w$  in their ground-truth are retrieved among the  $K$  nearest font shapes in the shared latent space. Formally,

$$P@K = \frac{1}{K} \sum_{i \in \Omega_{\text{test}}} \mathbf{1}(w \in \mathbf{W}_i) \cap \mathbf{1} \left( \|f(\mathbf{X}_i) - g(w)\| \leq \min_{i' \in \Omega_{\text{test}}} \|f(\mathbf{X}_{i'}) - g(w)\| \right), \quad (5)$$

where  $\mathbf{1}(\cdot)$  is the indicator function,  $\cap$  is the and-operation, and  $\min K$  is the operator to give the  $K$ th minimum value. Note that  $P@K$  is the evaluation for a *single* word query  $w$ . By the flexibility of DeepSets, it is possible to have a latent vector  $g(w)$  even for a single word  $w$ , although our method is trained with a set of impressions  $\mathbf{W}_i$  for each font  $i$ .

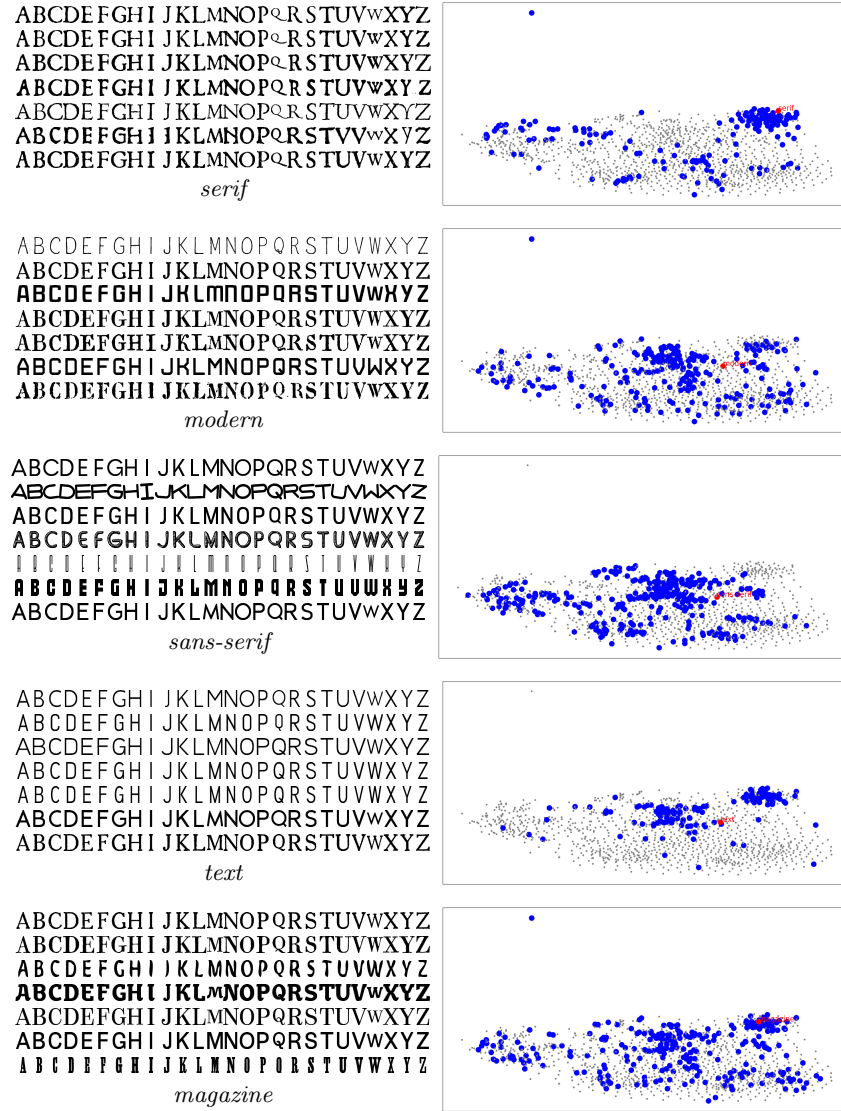


**Fig. 7.** tSNE visualization of the shared latent space for the words with  $P@10 \geq 0.5$ . Each dot corresponds to a font. A red dot corresponds to the impression word  $w$ . A blue dot corresponds to a font  $\mathbf{X}$  that the impression word  $w$  is attached as its ground-truth.

If  $P@K$  is 1, all the  $K$ -neighboring font shapes in the shared latent space have the impression word  $w$  in their ground-truth, and therefore the corresponding shape and word are embedded successfully while satisfying  $f(\mathbf{X}) \sim g(w)$ . If  $P@K$  is near or equal to zero, it means the corresponding word and shape are distant in the latent space. This might happen for the shape-irrelevant impression word.

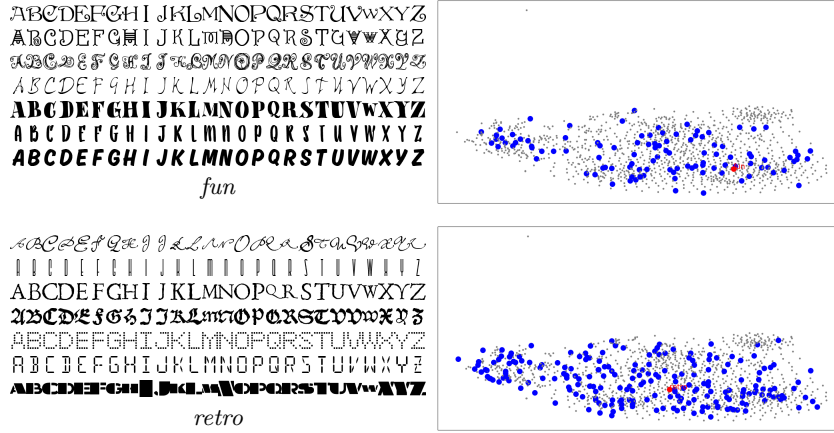


Fig. 8. tSNE visualization of the shared latent space for the words with  $P@10 = 0.1$ .

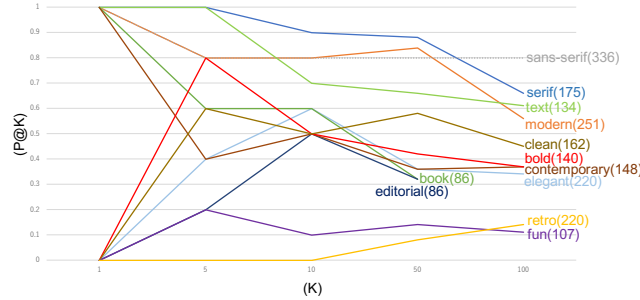


Fig. 9. The transition of  $P@K$  values along with  $K$  for several words.

Fig. 6 shows the lists of 18 words with higher  $P@10$ <sup>4</sup>. The list shows the font shape-relevant words, such as *serif*, *sans-serif*, *bold* and *condense*, as expected. This proves that our framework can learn the shared latent space successfully. It is noteworthy that the more subjective impression *elegant* has a high  $P@K$  value. Although the “elegance” of a font may vary among people, this result indicates there are common shape-relevant characteristics about it.

Fig. 7 visualizes the distribution of the test fonts in  $\Omega_{\text{test}}$  in the shared latent space by tSNE. We selected several impression words from Fig. 6 and plotted the tSNE of each word. On each tSNE of the word  $w$ , the latent vector  $f(\mathbf{X})$  of a font shape  $\mathbf{X}$  with the word  $w$  is depicted as a blue dot. The font shapes independent of  $w$  are depicted as gray dots. The red dot on tSNE corresponds to  $g(w)$ , that is, the latent vector of the impression word  $w$ . Since it is a “shared” latent space, we can plot the latent vectors of font shapes and impression words in the same space.

<sup>4</sup> Although *sans-serif* and *sans* might be the same, we use the original word tag in the MyFonts dataset.



Fig. 10. Generating images from single impression word.



Fig. 11. Generating images from multiple impression words.

Fig. 7 proves that the many appropriate font shapes (the blue dots) are gathering around  $g(w)$  (the red dot). This means that the corresponding shapes and words are embedded closely to each other in the shared latent space. At the same time, we can also observe that not all blue dots gather around  $g(w)$ . This suggests the diversity of the impression; the same impression word is attached to fonts with very different shapes. In other words, even for shape-relevant impression words, the font shape is not very similar, as shown in the font shape examples of *bold*.

Fig. 8 shows the tSNE visualization of the the latent vectors  $f(\mathbf{X})$  for more shape-irrelevant words, *fun* and *retro*. As expected from the above discussion on

the shape-relevant words, these shape-irrelevant words show far more scattered distributions; there is no condensation around  $g(w)$  even after co-training the shared latent space. In fact, P@10 of the two words is 0.1 (i.e., just one correct  $\mathbf{X}$  in the ten nearest neighbors). As shown in the font examples of *fun* and *retro*, the shape-irrelevant words do not correspond to a fixed font shape style, and therefore they do not show the condensation. Consequently, it is difficult to satisfy the condition  $f(\mathbf{X}) \sim g(w)$  for the shape-irrelevant word  $w$ .

Fig. 9 shows the transition of P@K values of several words along with  $K$ . The words are selected from the 18 words with higher P@10 (i.e., shape-relevant words) and two extra words, *retro* and *fun*. From this plot, it is possible to understand how the font shapes  $f(\mathbf{W})$  for each word spread in the latent space. Although less-frequent words have a handicap in P@K evaluation, some words, such as *sans-serif* and *fun*, keep the same P@K values between  $K = 10$  and 100 – this suggests they spread over from  $g(w)$  with almost the constant density.

### 5.3 Qualitative evaluation 2: Font image generation task

As shown in Fig. 5(b), we can use the shared latent space for generating font images with specific impressions. Using  $g(\mathbf{W}_i)$  as the input for the image decoder, we can get the alphabet images from ‘A’ to ‘Z’ at once. Theoretically, we can specify any impression words (even unlearned words). However, as we will see in the following experiment, the quality of the generated font images depends on the “type” of the impression words: shape-relevance and shape-irrelevance.

Fig. 10 shows the font generation results when a single impression word is given. For the shape-relevant words with higher P@10, i.e., *serif* to *condense*, legible font images with the specified impression are generated successfully, thanks to the property  $f(\mathbf{X}) \sim g(w)$ . However, for shape-irrelevant words, *fun* and *retro*, font images with just a neutral style were generated, due to their largely variable shapes, as shown in Fig. 8.

Fig. 11 shows the generation results when we specify multiple impression words. The result images generated by specifying two shape-relevant words become a mixed style successfully. The last example shows the case of the same words are specified two times; according to the property of DeepSets, we can strengthen an impression by this strategy.

### 5.4 Quantitative evaluation of the learned latent space

A quantitative evaluation is conducted by using the embedding results of all font data in  $\Omega_{\text{test}}$ . Specifically, we use an image retrieval scenario: Assume that we will give  $\mathbf{W}_i$  of the  $i$ th test font as a query. Then, all the images  $\mathbf{X} \in \Omega_{\text{test}}$  are then ranked by the distance  $\|f(\mathbf{X}) - g(\mathbf{W}_i)\|$ . Finally, the rank  $r_i$  of the correct image  $\mathbf{X}_i$  among  $|\Omega_{\text{test}}|$  images is determined. The average retrieval rank  $R_{t \rightarrow i} = \sum r_i / |\Omega_{\text{test}}|$  is the evaluation metric. Similarly, we have  $R_{i \rightarrow t}$  by exchanging  $\mathbf{W}_i$  and  $\mathbf{X} \in \Omega_{\text{test}}$  to  $\mathbf{X}_i$  and  $\mathbf{W} \in \Omega_{\text{test}}$ , respectively.

To our best knowledge, this is the first attempt at the cross-modal embedding of font impression and font shape into the shared latent space; therefore, there is

**Table 1.** Average retrieval rank. (\*: A similar setup to [21].)

Method	$R_{i \rightarrow t}$	$R_{t \rightarrow i}$
Independent	608.7	612.5
Image $\mapsto$ Text(*)	608.1	612.2
Text $\mapsto$ Image(*)	516.9	553.0
Proposed	<b>172.6</b>	<b>356.6</b>

no appropriate comparative baseline for this study. We, therefore, consider the following ablation cases to confirm the advantage of the proposed method.

- Proposed:  $f(\mathbf{X}_i)$  and  $g(\mathbf{W}_i)$  are embedded by the co-trained encoder (Section 4.3).
- Independent:  $f(\mathbf{X}_i)$  and  $g(\mathbf{W}_i)$  are embedded by the encoders by the initial training steps (Sections 4.1 and 4.2). No co-training has been made.
- Image  $\mapsto$  Text: After initializing the encoders, the encoder for the text modality is fixed. The encoder and decoder of the image modality are then trained so that  $f(\mathbf{X}_i) \sim g(\mathbf{W}_i)$ . This setup is very similar to a well-known previous research named cross-modal transfer [21].
- Text  $\mapsto$  Image: The opposite of the Image  $\mapsto$  Text setting. After initializing the encoder for the image modality, the encoder for the image modality is fixed. The encoder and decoder of the text modality are then trained so that  $f(\mathbf{X}_i) \sim g(\mathbf{W}_i)$ .

Table 1 shows the evaluation results. This indicates that the proposed method greatly outperformed the others. It also indicates that both Image  $\mapsto$  Text and Text  $\mapsto$  Image settings did not work well, which implies that joint optimization of cross-modal autoencoders was a key for obtaining meaningful shared representations.

## 6 Conclusion

This paper showed that it is possible to realize a shared latent space where a font shape image and its multiple impression words are embedded as similar vectors. Through the shared latent space, we can handle font shapes and their impressions in a unified manner, which can lead us to generate and retrieve font images with specific fonts and retrieve font images. Our various experimental results revealed the usefulness of the latent space. It is also clarified that the embedding quality depends on the shape-relevance of the impression words — it is rather reasonable because the latent space represents font shapes, as well as impression words.

## References

1. Almazán, J., Gordo, A., Fornés, A., Valveny, E.: Word spotting and recognition with embedded attributes. *IEEE Trans. Patt. Anal. Mach. Intell.* **36**(12), 2552–2566 (2014)

2. Biten, A.F., Tito, R., Mafla, A., Gomez, L., Rusinol, M., Valveny, E., Jawahar, C., Karatzas, D.: Scene text visual question answering. In: ICCV (2019)
3. Bojanowski, P., Grave, E., Joulin, A., Mikolov, T.: Enriching word vectors with subword information. *Trans. Assoc. Comput. Linguistics* **5**, 135–146 (2017)
4. Chen, T., Wang, Z., Xu, N., Jin, H., Luo, J.: Large-scale tag-based font retrieval with generative feature learning. In: ICCV (2019)
5. Childers, T.L., Jass, J.: All dressed up with something to say: Effects of typeface semantic associations on brand perceptions and consumer memory. *J. Consumer Psychology* **12**(2), 93–106 (2002)
6. Choi, S., Aizawa, K., Sebe, N.: Fontmatcher: Font image paring for harmonious digital graphic design. In: IUI (2018)
7. Doyle, J.R., Bottomley, P.A.: Mixed messages in brand names: Separating the impacts of letter shape from sound symbolism. *Psychology & Marketing* **28**(7), 749–762 (2011)
8. Fang, H., Gupta, S., Iandola, F., Srivastava, R.K., Deng, L., Dollár, P., Gao, J., He, X., Mitchell, M., Platt, J.C., et al.: From captions to visual concepts and back. In: CVPR (2015)
9. Haraguchi, D., Harada, S., Iwana Brian, K., Shinahara, Y., Uchida, S.: Character-independent font identification. In: DAS (2020)
10. Hayashi, H., Abe, K., Uchida, S.: GlyphGAN: Style-consistent font generation based on generative adversarial networks. *Knowledge-Based Syst.* **186** (2019)
11. Karpathy, A., Fei-Fei, L.: Deep visual-semantic alignments for generating image descriptions. In: CVPR (2015)
12. Lewis, C., Walker, P.: Typographic influences on reading. *British J. Psychology* **80**(2), 241–257 (1989)
13. Lyu, P., Bai, X., Yao, C., Zhu, Z., Huang, T., Liu, W.: Auto-encoder guided gan for chinese calligraphy synthesis. In: ICDAR (2017)
14. Mikolov, T., Sutskever, I., Chen, K., Corrado, G.S., Dean, J.: Distributed representations of words and phrases and their compositionality. In: NIPS (2013)
15. O'Donovan, P., Libeks, J., Agarwala, A., Hertzmann, A.: Exploratory font selection using crowdsourced attributes. *ACM Trans. Graphics* **33**(4), 92 (2014)
16. Saito, Y., Nakamura, T., Hachiya, H.: Exchangeable deep neural networks for set-to-set matching and learning. In: ECCV (2020)
17. Shaikh, D., Chaparro, B.: Perception of fonts: Perceived personality traits and appropriate uses. In: Digital Fonts and Reading, chap. 13. World Scientific (2016)
18. Shinahara, Y., Karamatsu, T., Harada, D., Yamaguchi, K., Uchida, S.: Serif or sans: Visual font analytics on book covers and online advertisements. In: ICDAR (2019)
19. Shirani, A., Dernoncourt, F., Echevarria, J., Asente, P., Lipka, N., Solorio, T.: Let Me Choose: From verbal context to font selection. In: ACL (2020)
20. Socher, R., Fei-Fei, L.: Connecting modalities: Semi-supervised segmentation and annotation of images using unaligned text corpora. In: CVPR (2010)
21. Socher, R., Ganjoo, M., Sridhar, H., Bastani, O., Manning, C.D., Ng, A.Y.: Zero-shot learning through cross-modal transfer. In: ICLR (2013)
22. Sumi, T., Iwana, B.K., Hayashi, H., Uchida, S.: Modality conversion of handwritten patterns by cross variational autoencoders. In: ICDAR (2019)
23. Vinyals, O., Toshev, A., Bengio, S., Erhan, D.: Show and tell: A neural image caption generator. In: CVPR (2015)
24. Wang, Y., Gao, Y., Lian, Z.: Attribute2Font. *ACM Trans. Graphics* **39**(4) (2020)
25. Wang, Z., Yang, J., Jin, H., Shechtman, E., Agarwala, A., Brandt, J., Huang, T.S.: DeepFont: Identify your font from an image. In: ACM Multimedia (2015)

26. Zaheer, M., Kottur, S., Ravanbakhsh, S., Póczos, B., Salakhutdinov, R., Smola, A.J.: Deep sets. In: NIPS (2017)
27. Zramdini, A., Ingold, R.: Optical font recognition using typographical features. IEEE Trans. Patt. Anal. Mach. Intell. **20**(8), 877–882 (1998)